

Clemson University

TigerPrints

All Theses

Theses

8-2022

Developing a Software Defined Radio Based Faraday Receiver

Alvaro J. Guerra
ajguerr@clemson.edu

Follow this and additional works at: https://tigerprints.clemson.edu/all_theses



Part of the [Engineering Physics Commons](#), and the [Other Physics Commons](#)

Recommended Citation

Guerra, Alvaro J., "Developing a Software Defined Radio Based Faraday Receiver" (2022). *All Theses*. 3895.

https://tigerprints.clemson.edu/all_theses/3895

This Thesis is brought to you for free and open access by the Theses at TigerPrints. It has been accepted for inclusion in All Theses by an authorized administrator of TigerPrints. For more information, please contact kokeefe@clemson.edu.

DEVELOPING A SOFTWARE DEFINED RADIO BASED FARADAY RECEIVER

A Thesis
Presented to
the Graduate School of
Clemson University

In Partial Fulfillment
of the Requirements for the Degree
Master of Science
Physics

by
Alvaro Javier Guerra
August 2022

Accepted by:
Dr. Stephen Kaeppler, Committee Chair
Dr. Gerald Lehmacher
Dr. Chad Sosolik

Abstract

The ionosphere can be approximated as a magnetized plasma. This results in wave-particle interactions driving a large quantity of ionospheric phenomena. To understand these phenomena, it is important to quantify and measure certain key plasma parameters. One such parameter is electron density. The Faraday Experiment was developed for the purpose of measuring electron density in the D-region of the ionosphere. This experiment was made popular by Martin Friedrich in the 1970s and is currently one of the only ways to provide high resolution measurements of electron density in the D-region without actively disturbing the surrounding plasma. This thesis aims to highlight this experiment and propose an update to one of its main components. This update would bring the Faraday Experiment up to date with today's technology and extend its usability. In this thesis, the history, methodology, and the development of the updated experiment will be discussed.

Dedication

This thesis was dedicated to my friends and family for helping and supporting me throughout this process.

Acknowledgments

Thank you to my all my committee members, mentors, and colleagues for helping me through this project.

Table of Contents

Title Page	i
Abstract	ii
Dedication	iii
Acknowledgments	iv
List of Figures	vi
1 Introduction	1
2 Background	4
2.1 Flight Heritage	5
2.2 Science Methodology	8
3 The Faraday Experiment	17
3.1 Mission Architecture	17
3.2 Concept of Operations	21
4 Motivation For Updating The Faraday Receiver	24
5 Building The SDR Based Faraday Receiver	26
5.1 Setting up the Hardware	26
5.2 Setting up the Software	28
6 Data Analysis	33
7 Conclusions	37
Appendices	38
A FaradayExperiment.grc	39
B gnu_autostart.py	55
C FaradayExperiment.py	56
Bibliography	60

List of Figures

2.1	Data from the Seddon Experiments showing Faraday Rotation [7].	6
2.2	Schematic of a Faraday Receiver from the McWave campaigns [3].	7
2.3	Faraday Receiver from one of the McWave campaigns [3].	8
2.4	Diagram showing Faraday Rotation versus vacuum propagation.	12
2.5	Polar Mesosphere Summer Echoes Observed by the MAARSY radar [8] . .	14
2.6	PMWE observed by the MAARSY radar in 2017 [5]	15
3.1	Faraday Experiment's mission Architecture	18
3.2	Plot comparing simulated magnetometer and single carrier frequency data	20
3.3	Seddon Experiment concept of operations.	21
3.4	Modern Faraday Experiment concept of operations	23
5.1	SDR based Faraday Experiment Hardware Components	27
5.2	Figure of the PAWSS payload	28
5.3	SDRplay Operating System image download page	29
5.4	UDP output of SDR Faraday Receiver from a 1KHz modulation on a 1.3MHz carrier	32
6.1	Simulated magnetometer data squared	34
6.2	Data from the CHAMPS mission [3]	35
6.3	Example of electron density profile from Faraday Experiment campaign 41.094 [3]	36

Chapter 1

Introduction

Due to its nature as a magnetized plasma, the ionosphere experiences many phenomena that are a result of charged particle interactions and electromagnetic wave dynamics. It is therefore crucial to understand and measure such interactions and dynamics. One of the most basic measurements we can make to characterize a plasma, is to measure its electron density. This is a fundamental property of a plasma as it defines many of its characteristics.

However, measuring electron density has its hurdles. While it is not a trivial task to measure electron density in the ionosphere, many have developed unique instruments and experiments that utilize our knowledge in plasma physics and electricity and magnetism in order to make measurements. However, most of these methods typically rely on observing the plasma's reaction to an imposed electric field, thus affecting the plasma of interest. There are but a few instruments that leave the plasma relatively undisturbed while measuring electron density. This thesis will describe one such instrument, The Faraday Receiver, as well as how it operates, the theory used to make the measurement, and how it can be improved in the future.

The Faraday Receiver is an instrument whose first iteration was inspired by the Seddon Experiment in the 1950s. This instrument was utilized in the later Faraday Experiment campaigns of the 1960s and has been used until recently in 2021. In order to

avoid future confusion it is important to emphasise the difference between the Faraday Receiver and the Faraday Experiment.

The Faraday Experiment was made popular by Martin Friedrich in the 1970s and has been one of the best ways to passively measure electron density in the D-region of the ionosphere. It refers to the experiment as a whole which utilizes the Faraday Receiver as one of its components.

This experiment has seen many updates and iterations in its lifespan and this thesis aims to add to this endeavor by proposing an improvement. Since its conception, this instrument has relied on the Faraday Effect. This effect causes a linearly polarized electromagnetic wave to rotate in its polarization plane when propagating through a magnetized plasma. This rotation of the polarization plane is proportional to the parallel magnetic field and electron density in the medium of propagation and can be used to determine these parameters. Chapter 2.2.2 detail how this instrument utilizes the property of Faraday Rotation to determine electron density in the ionosphere.

The experiment's main benefit has been that it can measure electron density while not disturbing the surrounding plasma. However, while the methodology and concept of operations remains sound, its current design does possess some issues. The current design was conceptualised around the 1960s and therefore requires 1960s technology which are no longer in production. There have been little to no component upgrades to the instruments since its original design. This has led to a slowdown in the utilization of this instrument as parts have become difficult to find. Chapter 4 will describe in detail why this is a problem and how to mitigate this issue by redesigning the instrument to be based on a Software Defined Radio (SDR) receiver.

The goal for this project was to update the Faraday Experiment by converting the Faraday Receiver to a SDR based instrument. This would allow for the continued use of the instrument and improve upon its current capabilities. This thesis will begin by describing the science behind the Faraday Experiment. Chapter 2.2.2 of this thesis will describe the flight history of the Faraday Experiment, the Faraday Effect and how it can

be applied to design an instrument to measure electron density in the ionosphere, as well as discuss a relevant phenomena whose understanding depends on the continuation of the Faraday Experiment. Chapter 3.2 will discuss the architecture of the Faraday Experiment and its concept of operations. Chapter 4 will discuss why the Faraday Receiver should be updated, what these updates consist of, and what it takes to convert it to software defined based. Chapter 5.2.2 will discuss the proposed updates and how they will be implemented. Chapter 6 will describe the data analysis process of deriving electron density from sounding rocket data.

Chapter 2

Background

When designing any scientific instrument, it is important to first understand what and why an instrument needs to be developed in the first place. Typically, there is a science question that the instrument attempts to address. For the Faraday Experiment, one of the science questions being addressed is how to measure electron density in the polar D-region of the atmosphere. Later section will discuss a phenomena known as Polar Mesosphere Winter Echoes (PMWEs), whose understanding requires the ability to measure electron density in the D-region with great resolution. In order to address the problem such an instrument must fulfill the following performance metrics and requirements:

1. Experiment shall measure electron density in the polar D-region
2. Measurements shall have an altitude resolution of 100m min
3. Experiment should not disturb the surrounding plasma
4. Experiment should fit in a standard sounding rocket payload deck

Meeting these requirements has allowed the Faraday Experiment to make progress in the understanding of various atmospheric phenomena since its first mission and it is still used today to provide electron density measurements for sounding rocket missions. This chapter will discuss the experiment's flight heritage, the science methodology behind the

Faraday Experiment, the concept of operations of the experiment, and a scientific use case.

2.1 Flight Heritage

In 1956, the Naval Research Lab (NRL) conducted an experiment that sought to measure electron density [7] in a new way. This experiment took advantage of the Faraday Effect as well as the innovations in High Frequency (HF) radio equipment of the time. This was the first ever iteration of what we now call the Faraday Experiment.

This first iteration made determining electron density profiles in the ionosphere while not disturbing the plasma possible. Past methods of measuring electron density profiles, such as Langmuir Probes, relied on charged probes that would disturb the plasma near the spacecraft. This can become an issue as one is actively modifying the background plasma. This type of instrument was also very susceptible to surface charging which is difficult to mitigate on a sounding rocket.

In contrast, the Seddon experiment made use of radio transmitters on-board the rocket along side dipole antennas, which would transmit several HF frequency signals down to ground receiver where the signal processing and data analysis would be done. This was done due to the computing limitations at the time.

Today we would fly the receivers onboard the rocket and transmit from the ground. We do this to reduce the amount of RF noise on the rocket itself, and thanks to the improvement in sounding rocket telemetry systems we are now able to do processing on the rocket and transmit the data product down to the ground. Figure 2.1 shows data from one of the Seddon experiments [7]. The first two signals in Figure 2.1 show the raw data from the ordinary and extraordinary signal modes from one frequency. One can see the rocket's spin modulated in the the data as well as the Faraday Rotation affecting the phase of both signals.

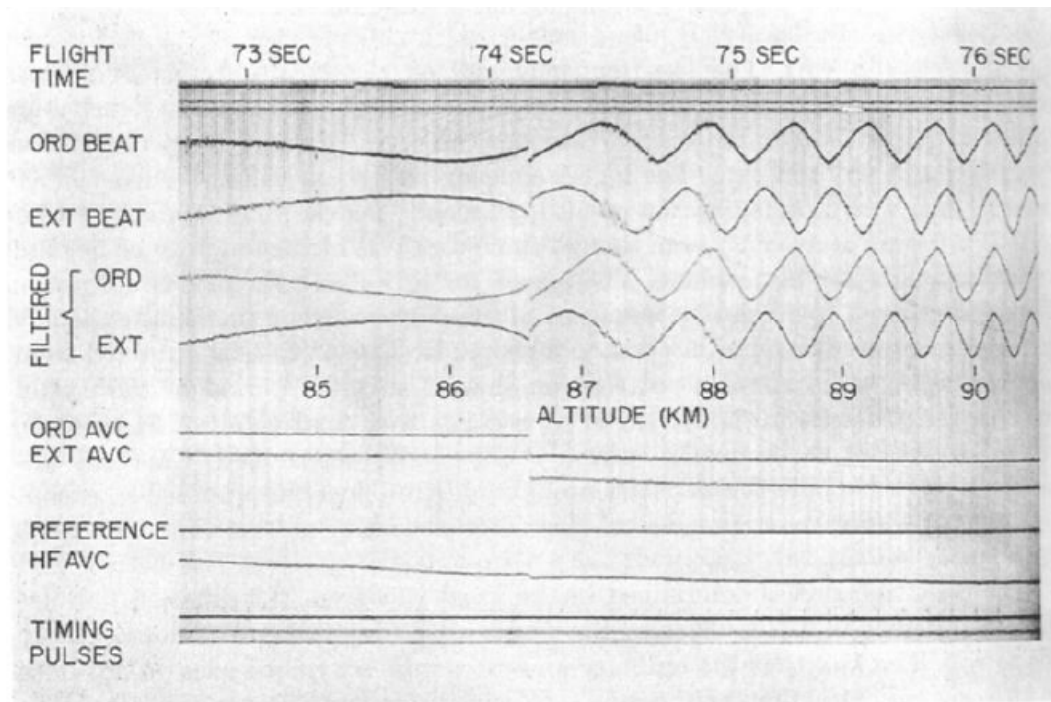


Figure 2.1: Data from the Seddon Experiments showing Faraday Rotation [7].

While the Seddon Experiment was the first iteration, the Faraday Experiment did not become what it is today until the late 1960s and 1970s. The experiment was popularized by Martin Friedrich in the 1970s [3] and has been flown on various sounding rocket missions all over the world. Friedrich miniaturized the instrument so as to be able to fly it on-board small sounding rockets growing the list of possible flight vehicles as well as reducing the cost per instrument.

2.1.1 The Analog Faraday Receiver Instrument Design

The Faraday receivers are based on analog AM radio receivers. While there have been many iterations of this instrument, they typically all fly four of these receivers. Figure 2.2 is a schematic of one of these receivers taken from Martin Friedrich's Handbook [3] and Figure 2.3 is a picture of the actual receiver board. This version of the receivers was used on the McWave campaigns in the early 2000s.

Each of these AM receivers are designed around the TCA 440 mixer chip and a local oscillator that tune a single frequency. This experiment requires four of these receivers in

order to tune to the four carrier frequencies. The four frequencies are specifically chosen to span the D-region of the ionosphere. This is necessary due to the signal reflection caused by the ionosphere. These frequencies are chosen so as to be affected by Faraday Rotation but as to not get reflected by the ionosphere. As both Faraday Rotation and total reflection are affected by electron density, there is only a small range in the HF frequency band that will meet the requirements in the D-region. The typical frequencies used are: 1.3, 2.3, 3.8, and 7.1 MHz. In order for each of the receivers to measure the same waveform signal, a low noise amplifier and a four way RF splitter is used. This allows for the use of only one dipole antenna. The following sections will go into detail about how these receivers measure the Faraday Rotation angle and how one derives electron density from that measurement.

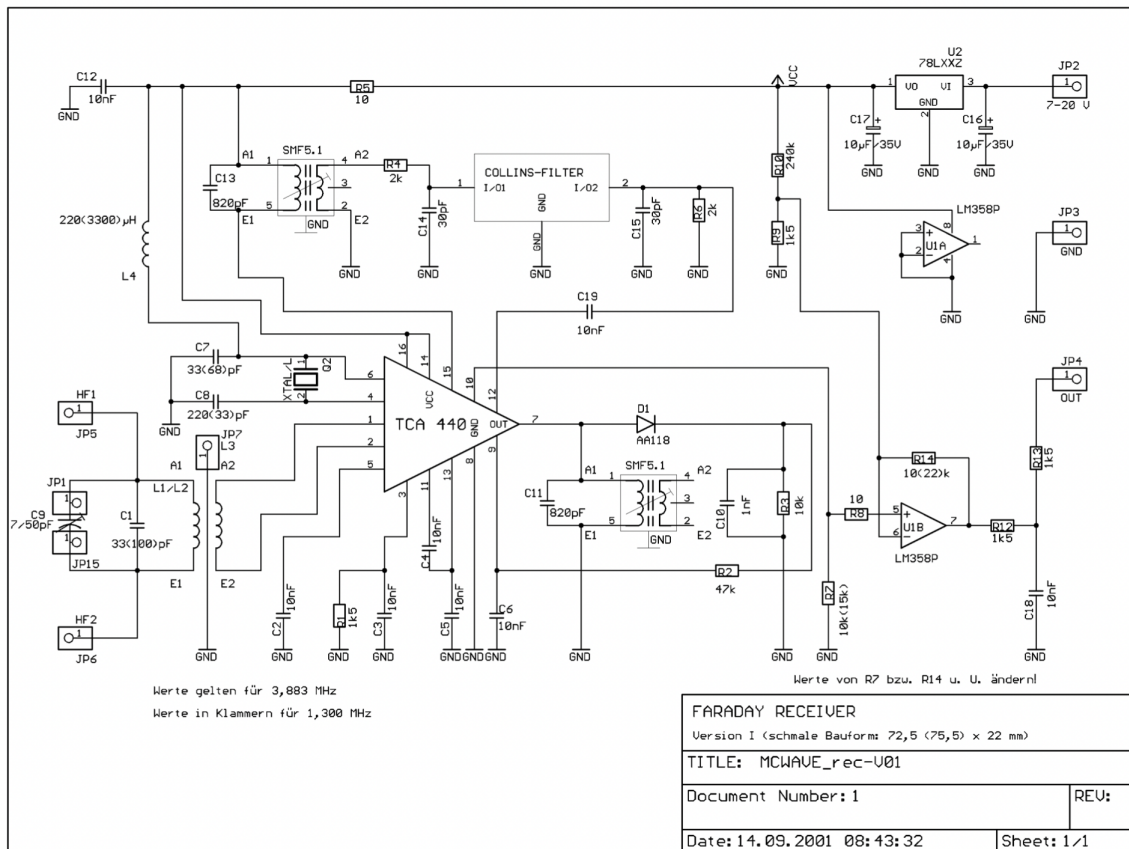


Figure 2.2: Schematic of a Faraday Receiver from the McWave campaigns [3].

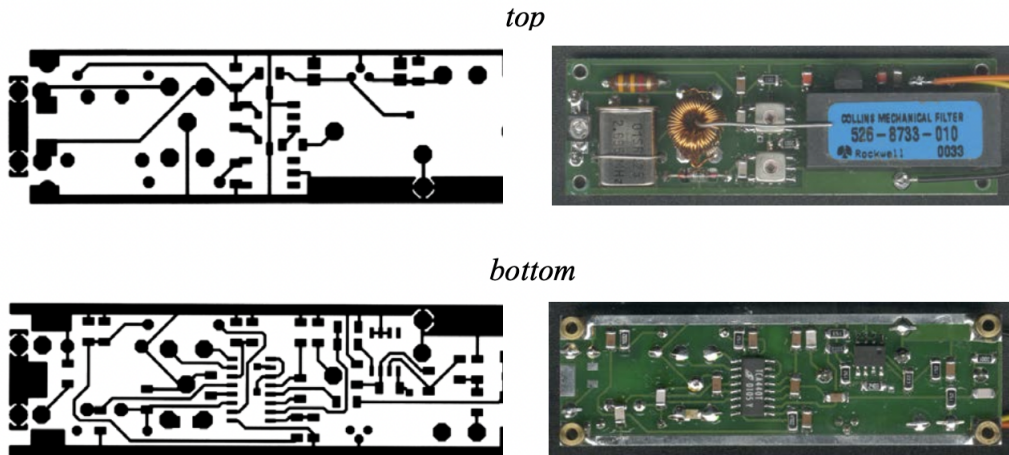


Figure 2.3: Faraday Receiver from one of the McWave campaigns [3].

2.2 Science Methodology

It has long been observed that, when propagating through a magnetized plasma, linearly polarized electromagnetic waves experience a rotation in their polarization angle. This effect was first discovered by Michael Faraday in 1845. It was significant as it was the first instance of an observation of light interacting with a magnetic field. This effect now goes by the name of the Faraday Effect or Faraday Rotation.

2.2.1 Faraday Rotation

The Faraday Effect, or Faraday Rotation, was discovered to be a result of electromagnetic wave interactions with embedded charges in mediums with a parallel external magnetic field. It was discovered by Michael Faraday in 1845. Today, we understand this effect as an interaction between free charges and electromagnetic fields. Previous to this discovery, the connection between light and electricity and magnetism had yet not been observed. Prior to this discovery light polarization had only been observed to be geometrically affected by passing through different mediums such as calcite crystals.

This effect has been used in many fields to measure and understand aspects of varying mediums such as the interstellar medium, the ionosphere, and laboratory plasmas.

In atmospheric physics we can use this effect to measure the electron density in the ionosphere. This section will describe how this effect manifests and the science behind it.

2.2.1.1 Circular Birefringence

Faraday Rotation is based on an optical property a material can possess that affects the plane of polarization of a linearly polarized electromagnetic wave. This optical property is called circular birefringence. However, prior to discussing circular birefringence it is useful for one to differentiate this phenomena from typical optical property of birefringence.

The typical optical birefringence is an optical property some materials hold, in which light rays of different polarization experience a different index of refraction as they propagate through said material. This property was discovered in the 1600s [1], a popular example of a material with this property is a calcite crystal. This crystal has a different index of refraction for horizontally and vertically polarized light. The difference in indices of refraction is typically attributed to an asymmetric crystalline structure. The asymmetry acts as a lens that can split light into its different polarization components. These types of materials have been used in the fields of optics and photography for the purpose of polarizing light sources and for imaging certain polarization of light for its property of redirecting the two types of polarization. This type of polarization only affects linearly polarized light due to its geometry.

Similarly, circular birefringence also affects with light polarization. Unlike typical birefringence, circular birefringence requires not only a specific medium, but also an external magnetic field in the direction parallel to the propagation direction of light. A material that holds this property is magnetized plasma. While not relying on geometric crystalline structures, magnetized plasma uses the interactions of free electrons and electromagnetic waves in order to create varying indices of refraction for circularly polarized light. This effect is called circular birefringence due to its effect on circularly polarized light. The circular birefringence effect causes right hand, $\vec{R}(z, t)$, and left hand, $\vec{L}(z, t)$,

circularly polarized electromagnetic waves to experience a different index of refraction. Unlike regular birefringence, a parallel magnetic field is required and the source of the difference in index of refraction is attributed to the amount of free moving electrons in the material and the magnitude of the parallel magnetic field. This effect causes the $\vec{L}(z, t)$ and $\vec{R}(z, t)$ waves to propagate at different speeds. Another difference is that, typical birefringence crystals physically separate and refract the horizontal and vertical polarization components, while circular birefringence changes propagation velocity and do not spatially separate the two polarization.

As one could expect, a circularly polarized electric field will cause an electron to move in a circular motion. From Ampere's law, we know that this moving electron will induce a magnetic field. This magnetic field will point in the direction perpendicular to the plane of polarization of the electric field and the rotating electron, therefore enhancing or attenuating the existing parallel magnetic field. One could picture this as a current loop with a magnetic field flowing through its center. If the background magnetic field is in the same or opposite direction as this induced magnetic field, it will have an effect on the free moving electron following the Lorentz force. This is the basis of the difference in the index of refraction for circularly polarized electric fields.

2.2.1.2 Rotation of the Polarization Axis

The connection between Faraday Rotation and linearly polarized light lies on the superposition principle. In classical mechanics we learn that a waveform can be broken down into its frequency components and by using Fourier analysis we can represent any waveform in terms of sines and cosines. Similarly, we can represent linearly polarized light in terms of circularly polarized light. In Quantum Mechanics we learn that we can create circularly polarized light by passing linearly polarized light through a 45° light polarizing filter [6]. Which can be represented by equation 2.1 from [6].

$$\vec{E}(z, t) = E_0 \frac{1}{\sqrt{2}} [(\cos(kz - \omega t)\hat{x} + \cos(kz - \omega t + \frac{\pi}{2})\hat{y})] \quad (2.1)$$

Similarly we can represent linearly polarized light as a sum of circularly polarized waves as is shown in equations 2.2.1.2.

$$\vec{R}(z, t) = E_0(\cos(k_r z - \omega t)\hat{x} + \sin(k_r z - \omega t)\hat{y})$$

$$\vec{L}(z, t) = E_0(\cos(k_l z - \omega t)\hat{x} - \sin(k_l z - \omega t)\hat{y}) \quad (2.2)$$

$$\vec{E}(z, t) = R + L = 2E_0\cos(kz - \omega t)\hat{x}$$

From equation 2.2.1.2, we observe that a linearly polarized electric field traveling in the \hat{z} direction, $\vec{E}(z, t)$, can be represented as a sum of circularly polarized electric fields. In vacuum, the $\vec{L}(z, t)$ and $\vec{R}(z, t)$ waves combine to create a linearly polarized wave with a constant polarization angle. However, circular birefringence causes these two circularly polarized waves to move at different speeds causing them to slowly shift out of phase. As the phase of the two waves shift further from zero, the polarization angle of the linearly polarized wave gets rotated. This is observed in a change in wavenumber, k , in the $\vec{L}(z, t)$ and $\vec{R}(z, t)$ waves. If $k_r \neq k_l$, then $\vec{E}(z, t)$ will no longer just be in \hat{x} but will now have a \hat{y} component as well. This relationship can be seen in Figure 2.4. The red in this figure corresponds to the polarization angle of an electric field in a magnetized plasma and the blue line corresponds to the polarization angle of an electric field propagating through vacuum. As the wave in the plasma propagates its angle of polarization will continue to increase until it reaches the starting point and will continue this circular motion until it exits the plasma.

The differential of this angle, $d\Omega$, can be characterized by the difference of index of refraction, μ_R and μ_L of the two circular modes, the angular frequency of the propagating wave, and the speed of light as can be seen equation 2.3 taken from [3].

$$d\Omega = \frac{\omega}{2c}(\mu_R - \mu_L)dz \quad (2.3)$$

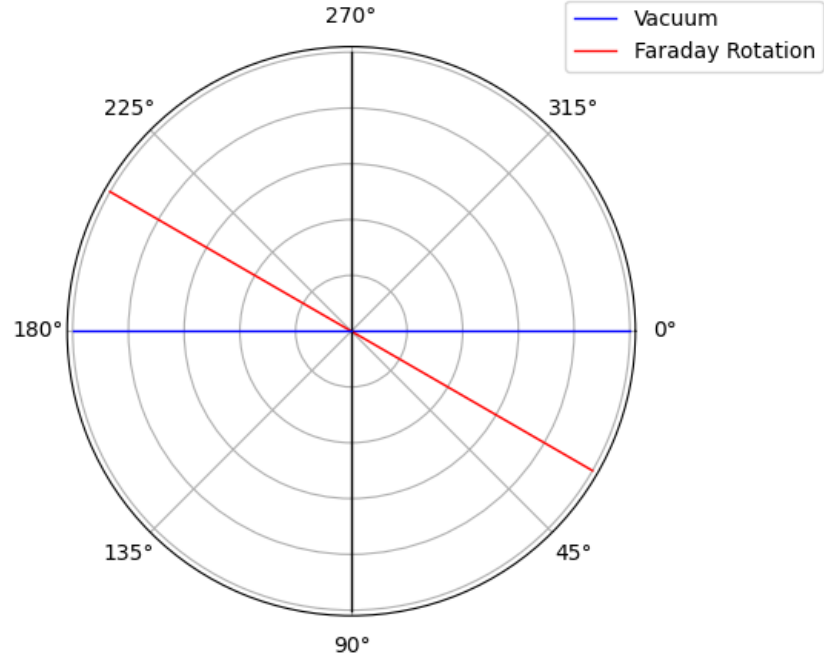


Figure 2.4: As a linearly polarized wave travels through a magnetized plasma, its angle of polarization will deviate in proportion to the electron density and the parallel magnetic field.

However, like previously discussed the Faraday effect in plasmas is primarily caused by the free electrons and a parallel magnetic field in the medium of propagation. Thus, it is more useful to obtain the Faraday Rotation angle in terms of those values. Equation 2.4 from [2] describes this relationship.

$$\Omega = \frac{e^3}{8\pi c \epsilon_0 m_e^2 f^2} \int_0^l n_e(z) B_z(z) dz \quad (2.4)$$

It is clear that one could now differentiate and invert to solve for electron density or the parallel magnetic field. This thesis will discuss the development of an instrument that takes advantage of this property and by measuring the Faraday Rotation angle and the parallel magnetic field, it is able to determine the electron density in the ionosphere.

2.2.2 Faraday Rotation and Polar Mesosphere Winter Echoes

As one could imagine, Faraday Rotation could be a great mechanism to determine electron density. The basis of the Faraday Experiment was to implement Faraday Rotation as a tool to measure this key component in the ionosphere. In the field of experimental Atmospheric and Space physics, measuring electron densities is very valuable. Since Earth's ionosphere is characterized as a magnetized plasma with a dipolar magnetic field, measuring its electron density can tell us a lot about its physical dynamics. A lot of phenomena in the upper atmosphere is driven by photo-ionization from the Sun and interactions with the magnetosphere. This results in electron density fluctuations which can drive a lot of different phenomena, One of these phenomena is known as Polar Mesosphere Winter Echoes (PMWEs). There has long been an interest for the discovery of the physical mechanism that drives these echoes, and to this day that remains a mystery. The PMWE campaigns [9] have been the most recent attempts to answer this question.

PMWEs present a great opportunity for the development of an instrument that can measure electron density near Earth's magnetic poles. These echoes are the winter counterpart to Polar Mesosphere Summer Echoes (PMSEs). Both of these echoes have been observed by the MAARSY radar located in Andøya, Norway [5] and have been studied for several decades. PMSEs typically reside at altitudes of 75-100 km (Figure 2.5), while PMWEs are typically found around 55-85 km (Figure 2.6). These echoes are a result of Bragg scatter reflections from radar soundings caused by electron density fluctuation structures in the order of the Bragg length of the radar. As these echoes are result of electron density fluctuations, it is important to measure, with high resolution, what these electron structures look like.

While PMSEs are thoroughly observed and understood, the drivers behind PMWEs are still unknown. PMSEs are very common and the conditions that cause them are ever-present in the summer months. Therefore, after much observation, it has been accepted that neutral air turbulence acting on ice particles is what is causing the electron structures to form [9]. PMWEs on the other hand, are much more elusive. As one can see

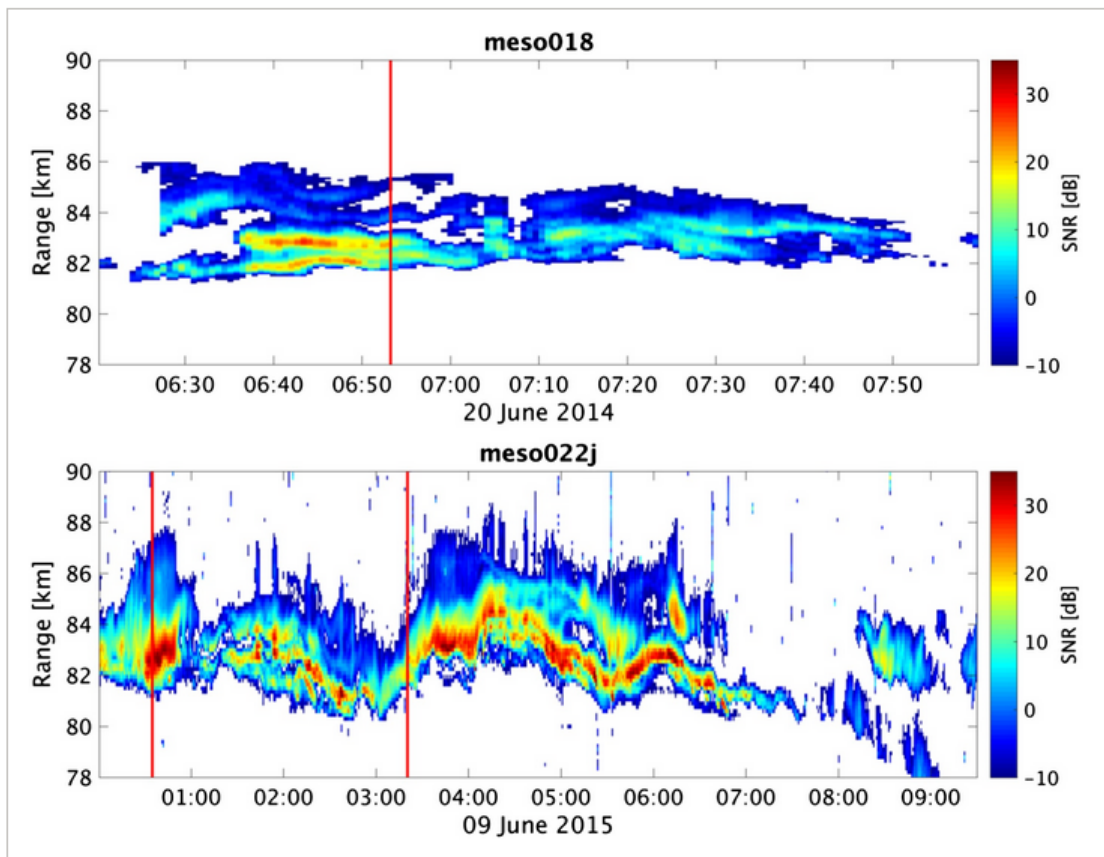


Figure 2.5: Polar Mesosphere Summer Echoes Observed by the MAARSY radar [8]

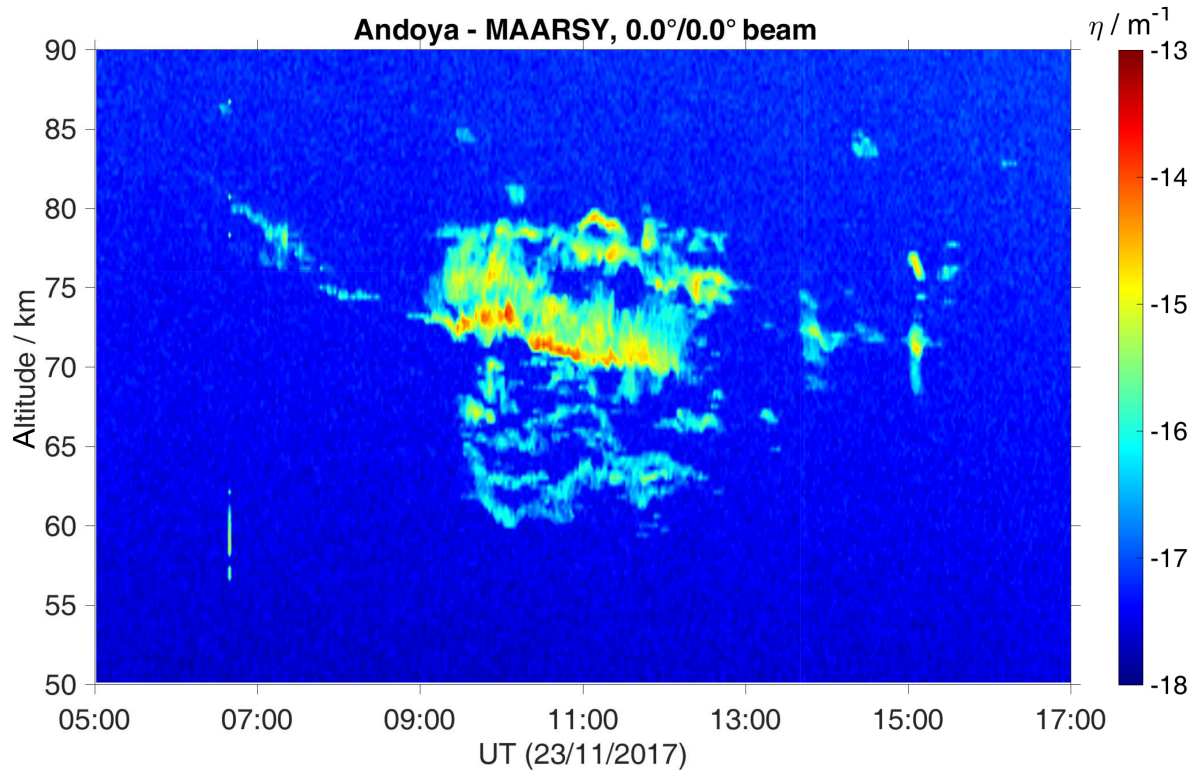


Figure 2.6: PMWE observed by the MAARSY radar in 2017 [5]

from Figure 2.6 PMWEs are have a shorter duration than PMSEs and are at a different altitude range. The conditions for the summer echoes do not exist in the winter as the D-region of the atmosphere is too warm for the ice particles to form. Therefore, the driver for PMWEs must be different than for PMSEs. There have been many theories that attempt to answer this question but more research is needed in order to form any conclusion.

One of the main tools used to study these echoes has been the analog Faraday Experiment. This experiment has provided electron density profiles during PMWE events which have helped in the understanding of the echoes. As these echoes are caused by electron structures it is crucial to measure the electron density fluctuations when searching for a driver of these echoes.

Since these echoes are present near Earth's magnetic poles, this presents a key advantage for the Faraday Experiment. The Faraday Effect relies on a parallel magnetic field and a medium of free electrons. Earth's poles meet these requirements. Earth's magnetic field is nearly vertical near the poles (in respect to the ground) and the ionosphere

is a large source of free charges. Therefore, a radio receiver on-board a sounding rocket launched and then pointed parallel to the magnetic field would observe Faraday Rotation when measuring a signal from a transmitter on the ground. If one is able to measure the polarization angle of the signal on the rocket, one would be able to integrate over distance and derive the line of sight total electron content. A differential in space can then be taken to determine the electron density. The following chapter will discuss such a mission and its concept of operations.

Chapter 3

The Faraday Experiment

This Chapter will describe the Faraday Experiment's mission architecture and concept of operations. As this experiment requires multiple instruments on the ground and on board the sounding rocket, it is helpful to split each of these into mission subsystems. The following section will describe these three subsystems and their components. The second section in this chapter will discuss the concept of operations of a mission that would utilize the Faraday Experiment. This section will describe how each subsystems fit into the grand scheme of the Faraday Experiment.

3.1 Mission Architecture

The Faraday Experiment can be broken down into three main subsystems as shown in Figure 3.1. These components can be sub-divided into two categories: rocket borne and ground based. The two rocket borne subsystems are the magnetometer subsystem and the Faraday Receiver subsystem. These two subsystems are both on-board the rocket but are independent of each other. The last subsystem is the ground station subsystem, which consists of the ground transmitters. This section will go over the fundamentals of each of the three subsystems.

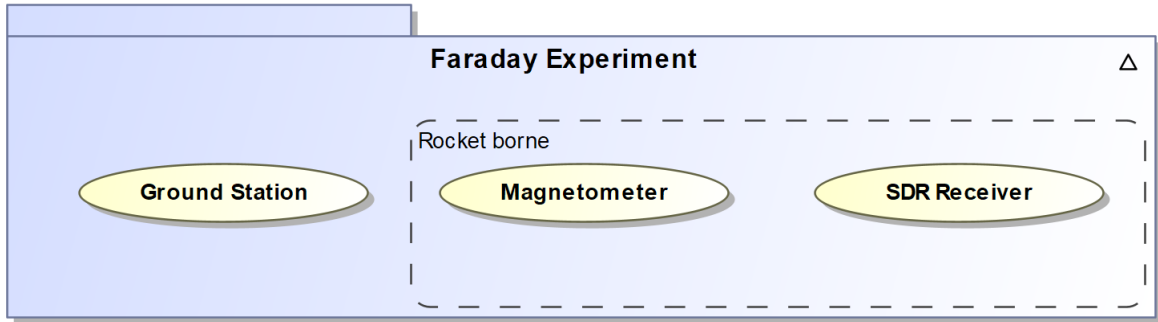


Figure 3.1: The Faraday Experiment’s mission architecture consists of the ground station, magnetometer, and SDR receiver subsystems

3.1.1 Ground Station Subsystem

The first subsystem we will discuss is the ground station subsystem. This subsystem is responsible for transmitting the desired carrier frequencies from the ground up to the payload. Its main components are the transmitters and antennas. The ground station comprises of four AM radio dipole antennas that each transmit a continuous waveform at a set frequency. Due to the long flight history of this experiment, the infrastructure for these ground stations is already existing in most of the world’s sounding rocket ranges.

When setting up the ground station antennas, it is important that the antennas be perpendicular to the rocket’s flight trajectory and parallel to the rocket borne antenna in order for this experiment to be successful. It is also ideal for these antennas to be off the ground and away from any RF emitting equipment.

As this experiment relies heavily on the use of Faraday rotation, it is crucial to choose frequencies that will be noticeably influenced by the ionosphere. The frequencies 1.3, 2.3, 3.8, and 7.1 MHz are nominally used for D- and E-region experiments. These frequencies were chosen based on the typical conditions of the D region. If chosen incorrectly, the frequencies could be experience total reflection or could experience more than one full rotation of their polarization angle which would both result in loss of data.

Magneto-ionic theory, tells us when the two modes, $\vec{L}(z, t)$ and $\vec{R}(z, t)$, will experience total reflection. When f , the signal frequency, equals the plasma frequency f_p ,

the $\vec{L}(z, t)$ will Experience total reflection. $\vec{R}(z, t)$ will experience a total reflection at $f=f_p+0.5f_c$. This property of total reflection can also be an aid while doing the data analysis, since if the point in which the signal experiences total reflection is known, then the plasma gyro frequency is also known at that point. This can serve as a post calibration and is one of the reasons to utilize multiple signal frequencies.

3.1.2 Magnetometer Subsystem

The second subsystem is somewhat optional and may be replaced with a high frequency signal that will be negligibly affected by Faraday Rotation. A carrier frequency of 132 MHz has been used for this purpose. Most sounding rockets already come equipped with an attitude control system magnetometer and thus another would be redundant. However, a carefully placed and calibrated magnetometer does have its benefits. It will not only be unaffected by Faraday Rotation, but also make it much easier to determine the rockets attitude for post launch data processing if the starting orientation is known.

The reason for this subsystem lies in that a magnetometer or a higher frequency carrier is necessary to determine the orientation of the rocket borne antenna with respect to the ground antenna. The full post launch processing will be discussed in a later section. However, one would presume that in vacuum, when the antennas are aligned one should expect a maximum in the power measured at the carrier frequency. By the same idea one should expect a minimum when the antennas are perpendicular. Meaning you don't experience Faraday Rotation. However, in the ionosphere this is not the case.

This is where the magnetometer subsystem comes in. Since the signal from the ground antenna passes through the ionosphere, it will experience Faraday Rotation. This will introduce a phase shift in the signal which will result in a maximum or minimum when the antennas are not aligned. The basis of this instrument lies in finding precisely what that phase shift is, as it will correspond to electron density in the ionosphere. The magnetometer will allow you to determine when you are physically aligned and aid in finding the Faraday Rotation angle.

The rocket's spin will modulate the received signals from the ground transmitters which can be observed as a phase shift in the measured signal. An exaggerated example can be observed in Figure 3.2. If aligned correctly, each of the maxima, in the magnetometer data, should correspond with a time in which the antennas are aligned and each minima when they are perpendicular. This can be used to determine the angle of the polarization plane of the incident wave. Chapter 6 will discuss how this is done.

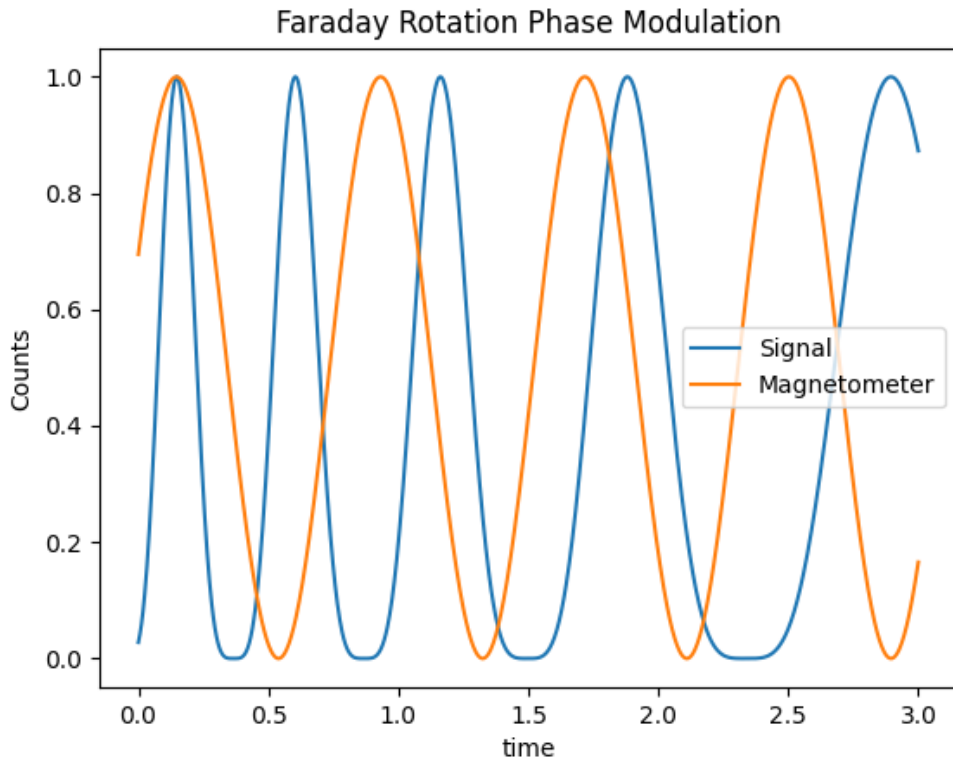


Figure 3.2: The signal from the ground experiences Faraday Rotation which manifests a phase shift, while the magnetometer reading does not experience this shift in phase.

3.1.3 Faraday Receiver Subsystem Design

The Faraday Receiver subsystem comprises of the rocket borne dipole antenna, a SDR, and a Raspberry Pi. The rocket borne antenna should be aligned perpendicularly to the axis of rotation of the rocket. For this proposed instrument, the RSPduo from SDRplay was chosen as the SDR. Along side a Raspberry Pi model 4B, the SDR and the

Raspberry Pi will be responsible for the command and data handling of the instrument. The dipole antenna must be connected to the RSPduo which then sends the IQ RF data to the Raspberry Pi for processing. The Raspberry Pi transmits the processed data to the sounding rocket telemetry system through the UDP protocol. The code running on the Raspberry Pi can be found in the Appendix of this thesis. The next chapter will go over how to setup both the hardware and software components of the Faraday Receiver subsystem.

3.2 Concept of Operations

The original radio based Faraday Experiment, had two main subsystems: the ground station and rocket payload. The ground station for the original experiment was a AM radio receiver and the rocket payload contained an AM transmitter. Figure 3.3 depicts the concept of operations of the first iteration of the Faraday Experiment. Later models switched to a rocket borne receiver and ground transmitter design which was determined to be a better design.

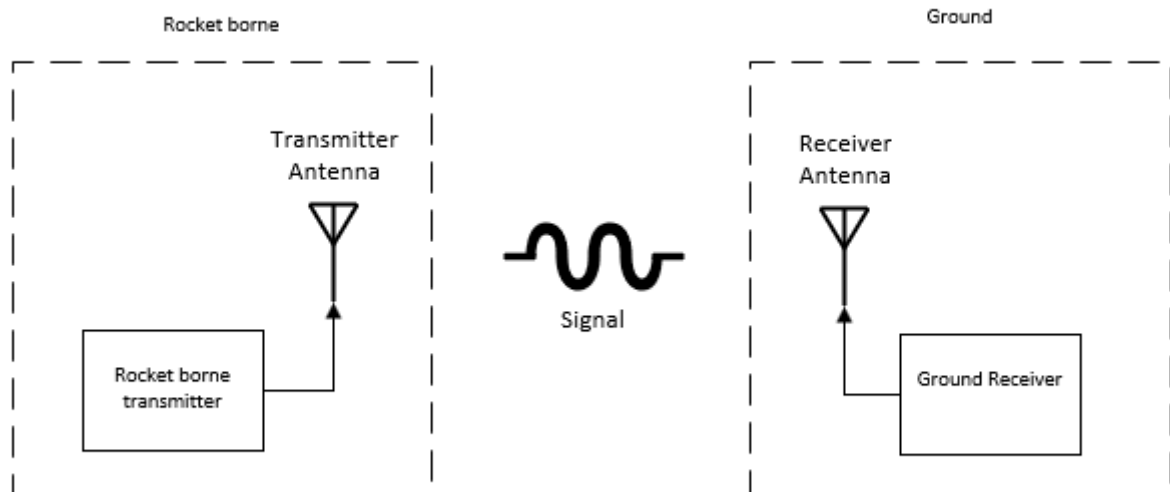


Figure 3.3: The original Faraday Experiment relied on a radio transmitter on-board the rocket that would transmit HF carrier signals down to the ground.

The current Faraday Experiment, as stated in the previous section, consists of three main subsystems. The concept of operations begins at the ground station subsystems. This subsystems makes use of four ground based HF transmitters to send the four carrier signals. These transmitters all have dipole antennas which provide the linearly polarized radio signals. These signals propagate through the ionosphere in a typical dipole pattern and their power is measured by the rocket's on-board receivers. As these signals propagate through the ionosphere they will experience Faraday Rotation. As the rocket spins, the signal power will be modulated at twice the spin frequency and the Faraday Rotation angle will manifest as a phase shift in the spin frequency. On the rocket, each of the four Faraday Receivers measures the same waveform. This waveform is a superposition of all four frequencies which must be filtered in order to measure the Faraday Rotation angle. Each of the four receivers tunes to one of the four carrier frequencies and measures the power at its corresponding frequency. These power measurements are compared to the on-board magnetometer in order to measure the Faraday Rotation angle. The procedure for doing this analysis will be discussed in Chapter 6.

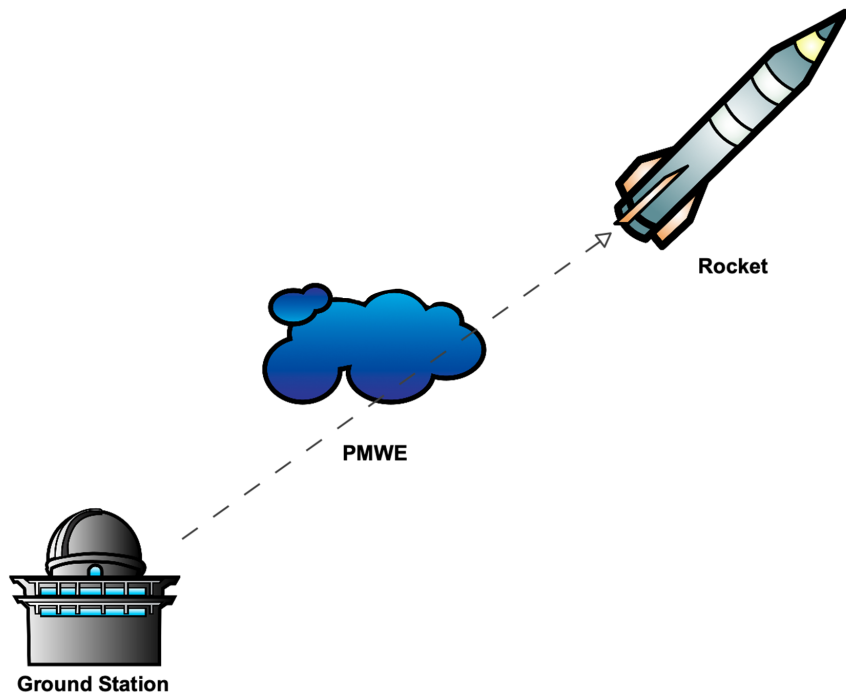


Figure 3.4: The current Faraday Experiment utilizes ground based transmitters and rocket borne receivers

Chapter 4

Motivation For Updating The Faraday Receiver

The main motivation for the switch to an SDR based Faraday Receiver stems primarily from the unavailability of the parts required to build the analog instrument. However, a switch to SDR based receivers will also result in added benefits.

It is clear that the Faraday Experiment, provides a measuring method that no other instrument can provide. It should hence be evident that the retiring of this experiment would be a detriment to the field of Atmospheric and Space Physics. This thesis aims to address an imminent scenario in which this experiment is no longer available. As previously stated part availability is the main issue. The main chip used in the analog receiver is the TCA 440 which is no longer in production. Similarly the Collins RF filters are very difficult to find and are also cost prohibitive. While in the past these components were viable, today they are no longer a sensible option.

This thesis hopes to provide another option for the Faraday Receiver. The hope is that by making the switch to SDR based receivers, the life of the experiment will be prolonged. In addition to switching to SDR based receivers, another option was considered. This option would be to redesign the analog receivers with modern analog components. While this option would work, it would not add anything new features to the existing

instrument. Ideally if this instrument was to be redesigned, the new version should have a better feature set. This led to the SDR solution being selected.

With the advent of powerful, small, and cheap single board computers as well as modern SDRs, the need for single purpose analog components has dwindled. Therefore, component manufacturers are no longer producing analog components at scale. Since industry is switching over software defined components, it only makes sense to update this instrument to take advantage of today's technologies.

An advantage to making the switch to SDR is added performance and modularity. Since with today's technology we are no longer constrained by computation power and telemetry limitations, a SDR based Faraday Receiver can provide a modularity and customization capabilities previously unavailable. Since the updated instrument contains a flight computer, it can be programmed to do onboard processing or to send all the raw data down to the ground. This was previously not possible as each of the receivers was only able to tune to a bandwidth of 300 Hz.

Another advantage of programming on the fly is that one does not have to make any hardware changes to switch frequencies. One could also reprogram the tuned frequencies by just uploading a new script rather than having to tune the analog system which would require special equipment and the disassembly and reassembly of the instrument housing.

Chapter 5

Building The SDR Based Faraday Receiver

This Chapter will describe how to set up the hardware and software for the updated Faraday Receiver. It will go over each hardware component and their interconnections as well as how to install and set up the software. This will be done for one Faraday Receiver, as each of the four is identical apart from the tuning frequency.

5.1 Setting up the Hardware

The set up for the SDR based Faraday Receiver is fairly straight forward. One of the benefits of switching to a SDR based instrument is the reduction of complexity and components. The only required components for a bench test prototype are an antenna with an SMA output, a Raspberry Pi model 4B (with a micro SD card), a RSPduo SDR, an Ethernet cable, and a USB B to A cable.

The bench setup of the Faraday Receiver can be seen in Figure 5.1. For testing, it would nominal to use the flight model in order to avoid performance issues. These hardware components are the backbone of the Faraday Receivers but in order to fly this on a sounding rocket one would need to design an enclosure and wiring harness specifically

made to interface with the flight vehicle. This updated receiver utilizes the UDP protocol for data communication to and from the sounding rocket and thus requires an Ethernet cable.

An example of a flight model can be seen in Figure 5.2. Simple aluminum rods or measuring tape can be used for the dipole antennas [3]. The four SDR subsystems can be stacked in a tower and the antenna passed through an RF splitter in order to send the signal to the four SDRs. The overall design for this instrument will vary depending on the implementation and flight vehicle but the components should remain a constant.

For the test setup, the antenna must be connected to the SDR through a SMA cable. The SDR needs to be connected to the Raspberry Pi's USB 3.0 port through a USB B to A cable. This instrument is setup to communicate through the UDP protocol so an Ethernet cable is required for data capture.

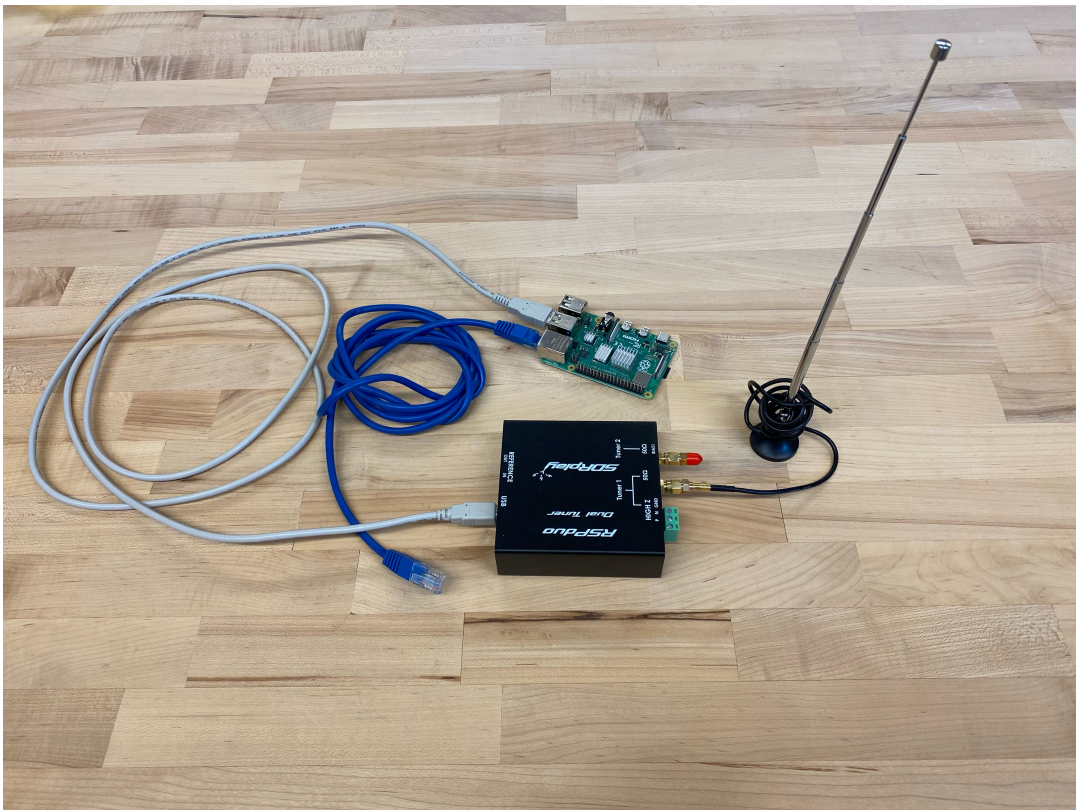


Figure 5.1: SDR based Faraday Experiment Hardware Components

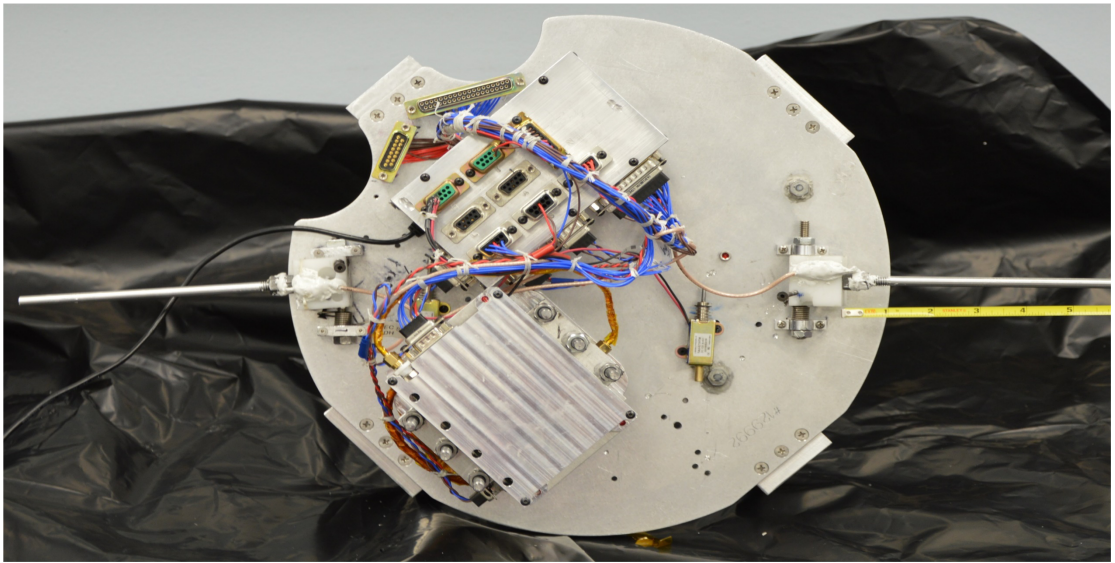


Figure 5.2: Example flight model for SDR based Faraday Receiver from PAWSS payload (G-Chaser campaign)

5.2 Setting up the Software

To set up the SDR based Faraday Receiver, one must first install the correct operating system on a micro SD card and insert it into the Raspberry Pi. The operating system used is a slightly modified version of the Raspberry Pi OS which is provided by SDRPlay. This Operating system contains all the required drivers for the RSPduo SDR to work properly.

5.2.1 Installing the Operating System

The required Operating System for this instrument is the SDRplay Raspberry Pi OS image. SDRplay has created a custom OS image that contains the dependencies and drivers for the gnuradio software to work properly and can be found on their website as well as full detailed instructions on installing it: <https://www.sdrplay.com/raspberry-pi-images/>. The correct image is the one on the left of the SDRplay website as can be seen in Figure 5.3. Different operating systems are not supported and may not work properly with the gnuradio script provided.

V0.6 IMAGE (RSP1, RSP1A, RSP2/2PRO, RSPDUO - SINGLE TUNER MODE)

This is the V0.6 release of the RPi image with SDRplay compatible software.

Note: During our testing using GQRX, we noticed high CPU load and some audio stuttering using RPi3B/+ with sample rates of greater than 500 kHz, so we recommend not using the RPi3 if you want to use GQRX. None of these issues were seen using the RPi4

The list of software on this image is: SoapySDR/SoapySDRPlay, SoapyRemote, Cubic SDR, GNU Radio Companion, GQRX, ADSB (Dump1090), QT-DAB receiver and the updated RSP TCP Server

List of known issues:

SoapyRemote

Will only work over LAN connections and locally. It will not work over Wide Area Networks

GQRX

Some limitations with tuner hardware control

Audio only via USB and HDMI audio

CPU load is quite high and may cause audio stuttering

Note: To use the TCP server, the ExtIO client plugin should be v1.1 and can be downloaded [here](#)

Download the image from here:

https://www.sdrplay.com/software/SDRplay_RPi_V0.6.img.xz

Checksum Information

Name: SDRplay_RPi_V0.6.img.xz

Size: 2395421684 bytes (2.23 GB)

SHA-256:

991EAC953DFC454BF0A8BA072BF805ED962B82619752A63AE3E6BDBD095DE4

Figure 5.3: SDRplay Operating System image download page

5.2.2 Setting up the gnuradio scripts

The basis for the on-board processing is based upon gnuradio [4] a python based software library that is used to develop for Software Defined Radio projects. The main script for this instrument was written with the use of the gnuradio_companion GUI application and exported as a python script. Gnuradio_companion serves as a great tool to set up each individual receiver and is what will be used to edit the scripts in order to select each of the tuning frequencies for the four receivers. Therefore, script provided in the Appendix requires the user to change the tuning frequency and IPaddress. This can all be done through the gnuradio_companion GUI.

In the Appendix of this thesis, you will find two scripts. One called, FaradayExperiment.grc and another called gnu_autostart.py. The provided gnuradio companion script named FaradayExperiment.grc will generate a python script called FaradayExperiment.py which is what would be used in a flight. If one is familiar with python and gnuradio, one could just edit the python script and avoid using gnuradio_companion all together. The FaradayExperiment.py is the main script that does the signal processing and data handling for the instrument. The gnu_autostart.py script initiates the FaradayExperiment.py script in order for the data collection to run after start up.

After the Raspberry Pi is booted, one can transfer the two scripts manually into the home directory of your pi `"/home/pi/"`. At this point one connects the Raspberry Pi to another computer via the Ethernet port. This instrument relies on the UDP protocol so a UDP capable device is required. On the Raspberry Pi, open up the terminal application and input the following command:

```
“gnuradio_companion FaradayExperiment.grc”
```

If the script is in your home directory, gnuradio should have opened with the correct script opened. At this point one should change the tuning frequency by clicking the on the variable box named tune and changing it to the desired carrier frequency in MHz. After the changes are made, generate the python script with the generate button.

At this point running the gnu_autostart.py in the terminal should start the Fara-

dayExperiment.py script and sending data. On another computer one can check to see if the Raspberry Pi is sending data by using the reader.py script provided in the appendix.

Once the instrument operating at the desired frequency, the autostart functionality must be enabled. After this step one will no longer be able to make any changes to the script as the Raspberry Pi will no longer boot to the desktop environment. To do so input the following commands into the terminal:

- `cd`
- `cp -r /etc/xdg/lxsession ~/.conf/`
- `echo @lxterminal >> ~/.conf/xdg/lxsession/LXD-Pi/autostart`

Now in the terminal one needs to setup a crontab to begin at startup using the following command: “`sudo crontab -e`”. This should give you a selection of editor, choose nano as the option. now write the following line:

“* * * * * `sudo python /home/pi/gnu_autostart.py &`”. After this, the setup is complete and the raspberry pi should start the script at bootup every time.

After the software has been installed, one should test the Faraday Receiver by inputting a modulated carrier signal into the RSPduo and checking the output through UDP. Figure 5.4 shows data captured from another Raspberry Pi over UDP when a 1.3MHz carrier modulated at 1KHz was sent through the RSPduo.

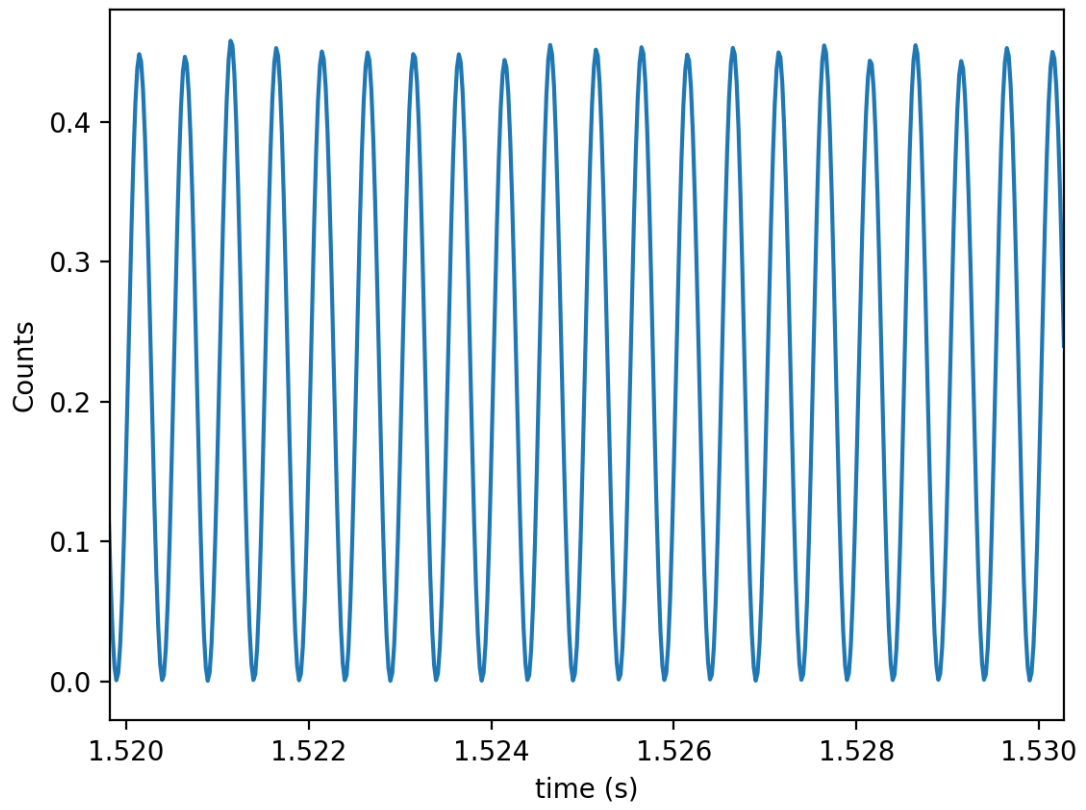


Figure 5.4: UDP output of SDR Faraday Receiver from a 1KHz modulation on a 1.3MHz carrier

Chapter 6

Data Analysis

In order to determine the Faraday Rotation of one of the carrier signals, one must know the attitude of the rocket antenna in respect to the ground antennas. Severe coning or tumbling will result in the carrier signal becoming unusable and thus the despinning of the rocket data becomes one of the most difficult steps. Having an unstable spin rate will therefore introduce errors in the Faraday rotation angle calculations. If we take a look at Figure 3.2, we can see that the magnetometer reaches a peak when aligned with the magnetic field and reaches a minimum when anti-parallel to the magnetic field. It is clear that the rocket's spin will also modulate the magnetometer at the rocket's roll rate. In vacuum the carrier signal's period would be half of the magnetometer. Since we are measuring power at each carrier frequencies, we do not know when we are aligned parallel or anti-parallel. Thus, the rockets roll rate experiences a doubling in frequency which can be observed in the data. The magnetometer measures the magnetic field direction so it is not subject to the frequency doubling. This problem can be easily mitigated by squaring the magnetic field measurements like in Figure 6.1.

We can now use the magnetometer to accurately determine the rockets attitude in respect to the ground transmitter. We then utilize equation 6.1 to determine the Faraday Rotation angle. This is done by measuring the power at each maximum, dividing it by

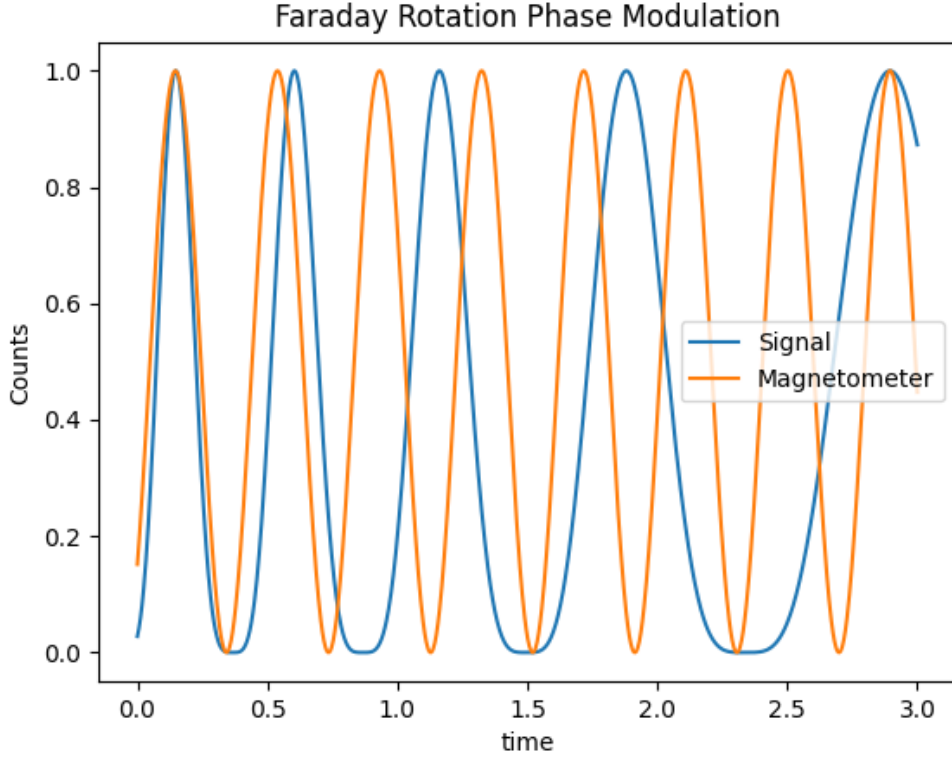


Figure 6.1: If we square the magnetic field we can identify the point when the antennas are aligned (maxima) and when the antennas are perpendicular (minima)

the power at each minimum and taking the inverse tangent of the quantity.

$$\tan(\Omega) \cong \frac{E_{EW}}{E_{NS}} \quad (6.1)$$

The proper alignment of the magnetometer is crucial to the mission. One issue that could arise is a misalignment between the magnetometer peak and antenna alignment. This could be mitigated by measuring the angle between the ground antennas and the rocket borne antenna as well as the magnetometer reading. After launch, a correction factor can be applied to the magnetometer data in order to properly align the data. One of the benefits with launching near the Earth's magnetic cusp, is the vertical magnetic field is predictable and fairly constant.

On a real flight the data will not look quite as nice as in Figure 6.1. In addition to the Faraday Effect, the ionosphere also has an absorption quality. This means that

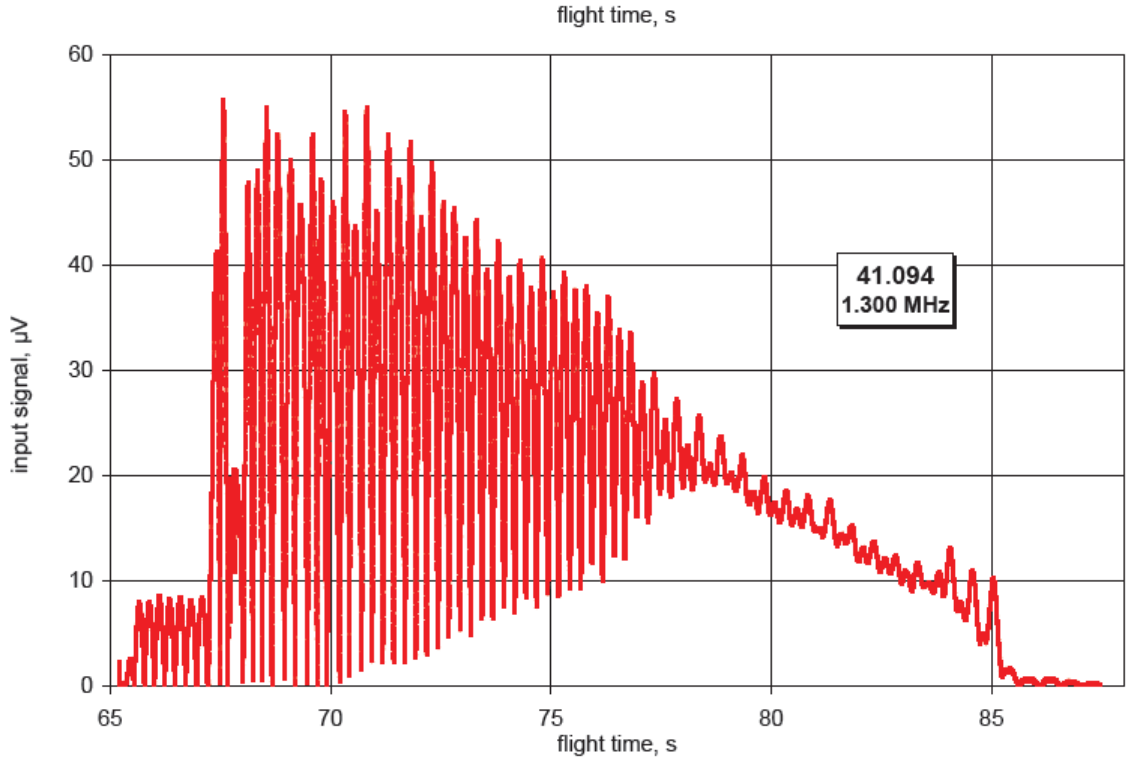


Figure 6.2: Data from the CHAMPS sounding rocket mission 41.094 from the University of Colorado [3]. This is the RAW data collected from the onboard receiver tuned to 1.3MHz.

your signal will be absorbed by the ionosphere, this absorption is highly dependent on the frequency of your signal and the distance away from the transmitter. This issue can be mitigated by choosing frequencies that will be only slightly affected and still experience Faraday Rotation. Example flight data from a past Faraday Experiment can be seen in Figure 6.2. This figure shows data from the CHAMPS campaign for the 1.3MHz receiver. As one can see as the rocket's altitude increase the peak-to-peak amplitude of the signal decreases. Past Faraday Experiments have mitigated this problem by utilizing four frequencies that can span all of the D-region.

$$\Omega = \frac{e^2}{8\pi^2 c \epsilon_0 m_e^2 f^2} \int_0^t n_e(z) B_z(z) dz \quad (6.2)$$

After the Faraday rotation angle is determined and have converted time to altitude, One can use equation 6.2 to determine the total electron content or by differentiating one

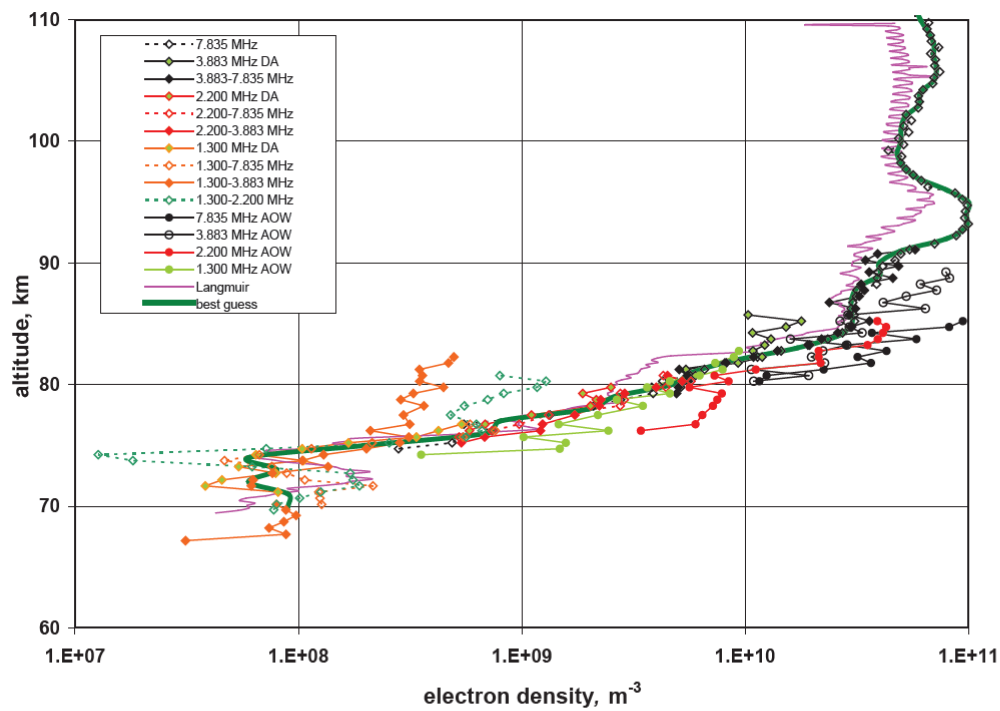


Figure 6.3: Example of electron density profile from Faraday Experiment campaign 41.094 [3]

can derive the electron density. Figure 6.3 shows data from the 41.094 campaign which compares electron density profiles from various data sources on the 41.094 flight.

Chapter 7

Conclusions

The Faraday Experiment has decades of flight heritage, and it provides a unique type of observation. Since its conception in the late 1950's, this experiment has gone through many design changes and iterations. However, the Faraday Experiment has not had an update since the late 1970s. This stagnation in innovation has led to a decline in its utilization. With the advent of cheap software defined radio technology it only makes sense to update the experiment. Given that one can purchase reliable cost effective software defined radios that can process more data than their analog counterparts, it is logical to make this upgrade.

The goal for this thesis was to provide a software defined radio based alternative to the analog Faraday Receiver. This update would replace the analog radio components with a SDR and a small single board computer like a Raspberry Pi. This will result in an instrument that is cost effective, easy to replicate, and modular.

This switch was greatly motivated by the current state of technology and the unavailability of analog radio components. In recent years it has been getting more and more difficult to obtain the necessary components to built this instrument. Analog filters and mixers are especially the problem. Therefore, by converting the instrument to software defined radio we can take this outdated instrument and bring it into the modern world.

Appendices

Appendix A FaradayExperiment.grc

```
<?xml version='1.0' encoding='utf-8'?>
<?grc format='1' created='3.7.13'?>
<flow_graph>
  <timestamp>Wed Mar 3 21:45:07 2021</timestamp>
  <block>
    <key>options</key>
    <param>
      <key>author</key>
      <value></value>
    </param>
    <param>
      <key>window_size</key>
      <value></value>
    </param>
    <param>
      <key>category</key>
      <value>[GRC Hier Blocks]</value>
    </param>
    <param>
      <key>comment</key>
      <value></value>
    </param>
    <param>
      <key>description</key>
      <value></value>
    </param>
```

```
<param>
  <key>_enabled </key>
  <value>True</value>
</param>
<param>
  <key>_coordinate </key>
  <value >(8, 8)</value>
</param>
<param>
  <key>_rotation </key>
  <value>0</value>
</param>
<param>
  <key>generate_options </key>
  <value>no_gui </value>
</param>
<param>
  <key>hier_block_src_path </key>
  <value >.:</value>
</param>
<param>
  <key>id </key>
  <value>FaradayExperiment2 </value>
</param>
<param>
  <key>max_nouts </key>
  <value>0</value>
</param>
```

```
<param>
  <key>qt_qss_theme </key>
  <value></value>
</param>
<param>
  <key>realtime_scheduling </key>
  <value></value>
</param>
<param>
  <key>run_command</key>
  <value>{python} -u {filename}</value>
</param>
<param>
  <key>run_options</key>
  <value>run</value>
</param>
<param>
  <key>run</key>
  <value>True</value>
</param>
<param>
  <key>sizing_mode </key>
  <value>fixed </value>
</param>
<param>
  <key>thread_safe_setters </key>
  <value></value>
</param>
```

```
<param>
  <key>title </key>
  <value></value>
</param>
<param>
  <key>placement </key>
  <value >(0,0)</value>
</param>
</block>
<block>
  <key>variable </key>
  <param>
    <key>comment</key>
    <value></value>
  </param>
  <param>
    <key>_enabled </key>
    <value>True</value>
  </param>
  <param>
    <key>_coordinate </key>
    <value >(272, 172)</value>
  </param>
  <param>
    <key>_rotation </key>
    <value>0</value>
  </param>
  <param>
```

```
<key>id</key>
  <value>decim</value>
</param>
<param>
  <key>value</key>
  <value>32</value>
</param>
</block>
<block>
  <key>variable</key>
  <param>
    <key>comment</key>
    <value></value>
  </param>
  <param>
    <key>_enabled</key>
    <value>True</value>
  </param>
  <param>
    <key>_coordinate</key>
    <value>(8, 160)</value>
  </param>
  <param>
    <key>_rotation</key>
    <value>0</value>
  </param>
  <param>
    <key>id</key>
```

```
    <value>samp_rate</value>
</param>
<param>
    <key>value</key>
    <value>48*32e3</value>
</param>
</block>
<block>
    <key>variable</key>
    <param>
        <key>comment</key>
        <value></value>
    </param>
    <param>
        <key>_enabled</key>
        <value>True</value>
    </param>
    <param>
        <key>_coordinate</key>
        <value>(400, 176)</value>
    </param>
    <param>
        <key>_rotation</key>
        <value>0</value>
    </param>
    <param>
        <key>id</key>
        <value>tune</value>
```

```
</param>
<param>
  <key>value</key>
  <value>1.3e6</value>
</param>
</block>
<block>
  <key>band_pass_filter</key>
  <param>
    <key>beta</key>
    <value>6.76</value>
  </param>
  <param>
    <key>alias</key>
    <value></value>
  </param>
  <param>
    <key>comment</key>
    <value></value>
  </param>
  <param>
    <key>affinity</key>
    <value></value>
  </param>
  <param>
    <key>decim</key>
    <value>32</value>
  </param>
```



```
<param>
  <key>_enabled </key>
  <value>True</value>
</param>
<param>
  <key>type</key>
  <value>fir_filter_ccf </value>
</param>
<param>
  <key>_coordinate </key>
  <value>(376, 460)</value>
</param>
<param>
  <key>_rotation </key>
  <value>0</value>
</param>
<param>
  <key>gain</key>
  <value>2</value>
</param>
<param>
  <key>high_cutoff_freq </key>
  <value>1.2e3</value>
</param>
<param>
  <key>id</key>
  <value>band_pass_filter_0 </value>
</param>
```

```
<param>
  <key>interp </key>
  <value>1</value>
</param>
<param>
  <key>low_cutoff_freq </key>
  <value>800</value>
</param>
<param>
  <key>maxoutbuf</key>
  <value>0</value>
</param>
<param>
  <key>minoutbuf</key>
  <value>0</value>
</param>
<param>
  <key>samp_rate</key>
  <value>samp_rate</value>
</param>
<param>
  <key>width</key>
  <value>300</value>
</param>
<param>
  <key>win</key>
  <value>fir_des.WIN_HAMMING</value>
</param>
```

```
</block>
<block>
  <key>blocks_udp_sink </key>
  <param>
    <key>alias </key>
    <value></value>
  </param>
  <param>
    <key>comment</key>
    <value></value>
  </param>
  <param>
    <key>affinity </key>
    <value></value>
  </param>
  <param>
    <key>ipaddr </key>
    <value>169.254.208.61 </value>
  </param>
  <param>
    <key>port </key>
    <value>6666</value>
  </param>
  <param>
    <key>_enabled </key>
    <value>True</value>
  </param>
  <param>
```

```
<key>_coordinate</key>
  <value>(680, 516)</value>
</param>
<param>
  <key>_rotation</key>
  <value>0</value>
</param>
<param>
  <key>id</key>
  <value>blocks_udp_sink_0</value>
</param>
<param>
  <key>type</key>
  <value>complex</value>
</param>
<param>
  <key>psize</key>
  <value>8192</value>
</param>
<param>
  <key>eof</key>
  <value>True</value>
</param>
<param>
  <key>vlen</key>
  <value>1</value>
</param>
</block>
```

```
<block>
  <key>sdrplay_rspduo_source </key>
  <param>
    <key>agc_enabled </key>
    <value>True</value>
  </param>
  <param>
    <key>antenna </key>
    <value>'T2_50ohm'</value>
  </param>
  <param>
    <key>bw</key>
    <value>1536</value>
  </param>
  <param>
    <key>biasT </key>
    <value>False </value>
  </param>
  <param>
    <key>alias </key>
    <value></value>
  </param>
  <param>
    <key>bcast_notch </key>
    <value>False </value>
  </param>
  <param>
    <key>comment</key>
```

```
<value></value>
</param>
<param>
  <key>affinity </key>
  <value></value>
</param>
<param>
  <key>dab_notch </key>
  <value>False </value>
</param>
<param>
  <key>dc_offset_mode </key>
  <value>True </value>
</param>
<param>
  <key>debug_enabled </key>
  <value>False </value>
</param>
<param>
  <key>device_serial </key>
  <value>'0' </value>
</param>
<param>
  <key>_enabled </key>
  <value>True </value>
</param>
<param>
  <key>_coordinate </key>
```

```
<value >(16, 284)</value>
</param>
<param>
  <key>_rotation </key>
  <value>0</value>
</param>
<param>
  <key>id </key>
  <value>sdrplay_rspduo_source_0 </value>
</param>
<param>
  <key>if_atten_db </key>
  <value>40</value>
</param>
<param>
  <key>ifType </key>
  <value>0</value>
</param>
<param>
  <key>iq_balance_mode </key>
  <value>False </value>
</param>
<param>
  <key>lna_atten_step </key>
  <value>0</value>
</param>
<param>
  <key>lo_mode </key>
```

```

    <value>1</value>
</param>
<param>
    <key>maxoutbuf</key>
    <value>0</value>
</param>
<param>
    <key>minoutbuf</key>
    <value>0</value>
</param>
<param>
    <key>rf_freq</key>
    <value>tune</value>
</param>
<param>
    <key>sample_rate</key>
    <value>samp_rate</value>
</param>
</block>
<connection>
    <source_block_id>band_pass_filter_0</source_block_id>
    <sink_block_id>blocks_udp_sink_0</sink_block_id>
    <source_key>0</source_key>
    <sink_key>0</sink_key>
</connection>
<connection>
    <source_block_id>sdrplay_rspduo_source_0</source_block_id>
    <sink_block_id>band_pass_filter_0</sink_block_id>

```



```
<source_key>0</source_key>  
<sink_key>0</sink_key>  
</connection>  
</flow_graph>
```

Appendix B gnu_autostart.py

```
import FaradayExperiment

def my_main(top_block_cls=FaradayExperiment.FaradayExperiment,
            options=None):
    tb = top_block_cls()
    tb.start()
    tb.wait()
if __name__ == '__main__':
    my_main()
```

Appendix C FaradayExperiment.py

```
#!/usr/bin/env python2
# -*- coding: utf-8 -*-
#####
# GNU Radio Python Flow Graph
# Title: Faradayexperiment
# Generated: Wed Mar  3 21:52:33 2021
#####

from gnuradio import blocks
from gnuradio import eng_notation
from gnuradio import filter
from gnuradio import gr
from gnuradio.eng_option import eng_option
from gnuradio.filter import firdes
from optparse import OptionParser
import sdrplay

class FaradayExperiment(gr.top_block):

    def __init__(self):
        gr.top_block.__init__(self, "Faradayexperiment")

        #####
        # Variables
```

```

#####
self.tune = tune = 1.3e6
self.samp_rate = samp_rate = 48*32e3
self.decim = decim = 32

#####

# Blocks

#####

self.sdrplay_rspduo_source_0 = sdrplay_rspduo_source(tune,
    1536, True, 40, True, False,
    False, 0, 1, samp_rate, False, False, 0, False,
    '0', 'T2_50ohm')

self.blocks_udp_sink_0 = blocks_udp_sink(gr.sizeof_gr_complex*1,
    '169.254.208.61', 6666, 8192, True)
self.band_pass_filter_0 = filter_fir_filter_ccf(32,
    firdes.band_pass(2, samp_rate, 1, 1.2e3, 300,
    firdes.WIN_HAMMING, 6.76))

#####

# Connections

#####

self.connect((self.band_pass_filter_0, 0),
    (self.blocks_udp_sink_0, 0))
self.connect((self.sdrplay_rspduo_source_0, 0),
    (self.band_pass_filter_0, 0))

```

```

def get_tune(self):
    return self.tune

def set_tune(self, tune):
    self.tune = tune
    self.sdrplay_rspduo_source_0.set_rf_freq(self.tune)

def get_samp_rate(self):
    return self.samp_rate

def set_samp_rate(self, samp_rate):
    self.samp_rate = samp_rate
    self.band_pass_filter_0.set_taps(firdes.band_pass(2,
        self.samp_rate, 1, 1.2e3, 300, firdes.WIN_HAMMING, 6.76))

def get_decim(self):
    return self.decim

def set_decim(self, decim):
    self.decim = decim

def main(top_block_cls=FaradayExperiment, options=None):

    tb = top_block_cls()
    tb.start()
    tb.wait()

```

```
if __name__ == '__main__':  
    main()
```

Bibliography

- [1] R. Bartholin. *Experimenta Crystalli Islandici disdiacastici, quibus mira et insolita refractio detegitur*. 1669.
- [2] F.D.G. Bennett, J.E. Hall, and P.H.G. Dickinson. D-region electron densities and collision frequencies from faraday rotation and differential absorption measurements. *Journal of Atmospheric and Terrestrial Physics*, 34(8):1321–1335, 1972.
- [3] Martin Friedrich. *Handbook of the Lower Ionosphere*. Verlag der Technischen Universität Graz, 200 edition, October 2016.
- [4] GNU Radio Website, accessed March 2022.
- [5] R. Latteck, T. Renkwitz, and B. Strelnikov. D region observations by vhf and hf radars during a rocket campaign at andøya dedicated to investigations of pmwe. *Advances in Radio Science*, 17:225–237, 2019.
- [6] J. J. Sakurai and Jim Napolitano. *Modern Quantum Mechanics*. Cambridge University Press, 2 edition, 2017.
- [7] J. Carl Seddon. Differential absorption in the d and lowers-e regions. *Journal of Geophysical Research (1896-1977)*, 63(1):209–216, 1958.
- [8] Svenja Sommer, Jorge L. Chau, and Carsten Schult. On high time-range resolution observations of pmse: Statistical characteristics. *Journal of Geophysical Research: Atmospheres*, 121(12):6713–6722.
- [9] Boris Strelnikov, Tristan Staszak, Ralph Latteck, Toralf Renkwitz, Irina Strelnikova, Franz-Josef Lübken, Gerd Baumgarten, Jens Fiedler, Jorge L. Chau, Joan Stude, Markus Rapp, Martin Friedrich, Jörg Gumbel, Jonas Hedin, Evgenia Belova, Marcus Hörschgen-Eggers, Gabriel Giono, Igor Hörner, Stefan Löhle, Martin Eberhart, and Stefanos Fasoulas. Sounding rocket project “pmwe” for investigation of polar mesosphere winter echoes. *Journal of Atmospheric and Solar-Terrestrial Physics*, 218:105596, 2021.